

Anatomical Shape Reconstruction and Manufacturing: solving topological changes of lumen vessel through geometric approach

Fabrizio Murgia*, Gabriella Pusceddu*,
Gregorio Franzoni*, Piero Pili*

*CRS4, EIP/GEMS Area

Parco Scientifico e Tecnologico, POLARIS
Edificio 1, 09010 PULA (CA), Italy
tel +39 07092501
fax +39 0709250216
Email: piero.pili@crs4.it

Massimiliano Tuveri†

†Vascular Surgery Dept. Ospedale Sant'Elena,
Via Marconi 160, 09045 Quartu Sant'Elena (CA), Italy

Abstract—Over the last years there has been an increasing growth of interest in Rapid Prototyping (RP) techniques applied to various fields of medicine. RP makes it possible, in vascular surgery, to produce accurate anatomic replicas of patient vessels. These replicas can help the customization of surgical invasive interventions such as in situ stent-graft insertion in carotid region.

The main goal of this work is to obtain high quality in lumen reconstruction and manufacturing replicas by RP technique. This goal is achieved through the complete control of each phase of the generating process.

We present a semi-automatic method for carotid lumen reconstruction based on Boundary Representation (BRep). All parameters influencing the quality of the shape reconstruction are presented and discussed: shape acquisition, shape reconstruction and shape manufacturing. The shape acquisition starts by extracting the points belonging to the boundary of the lumen vessel, from Computer Tomography (CT) images. These points, parameterised in a vector, are the input data of the shape reconstruction algorithm based on B-Spline interpolation. The B-Spline type for representing curves and surfaces were chosen because of their properties of continuity and local control.

In the shape reconstruction stage we had to face problems due to the topological change on the vessel structure. For vessel regions where there are not changes of topology, we use the closed B-Spline curves (belonging to adjacent acquisition planes) as generating curves to build a B-Spline surface. For vessel regions with at least a change of topology (ex. bifurcation region) our algorithm split automatically the involved curves to obtain three rectangular B-Spline patches. Such patches are joined together to obtain the bifurcation vessel lumen. The set of lumen surfaces is then inserted in a Boundary Representation in order to get a valid solid.

To analyse the quality of the reconstructed shapes, the final object is compared with the acquisition image. This solid is correctly tessellated in triangles to produce the data format used by the RP devices (STL).

Keywords: Boundary Representation, Reconstruction, B-Spline, Topology, Rapid Prototyping.

I. INTRODUCTION

In 1991, a study of Parodi et al. [1] reports for the first time on animal experimentation and initial clinical trials exploring the feasibility of excluding of an abdominal aortic aneurysm by placing of an intraluminal, stent-anchored, Dacron prosthetic graft (stent-graft).

The stent-graft device is cylinder-shaped, mesh-like metal scaffolding, usually coated with plastic or "fabric" material, that an interventional radiologist can place within a channel to keep it open. When compressed and fitted onto a catheter, the stent-graft can be inserted through a small femoral arteriotomy, or possibly percutaneously. When released from the catheter, the stent-graft expands to a size and shape, pre-determined, during the planning stage, providing a new normal-sized lumen to maintain blood flow. Anatomically correct positioning of appropriately sized stents does not produce relevant flow disturbances in the Internal Carotid Artery (ICA) (see Fig. 1). For clinical application, stent location and size must be carefully determined [2]. The stent-graft is designed to fit tightly into the blood vessel, creating a pressure seal that prevents flow around the stent-graft [3]. Sometimes after the stent insertion some leaks are found. Main causes of leaks are: misplacement of the stent-graft; morphologic features of the vessel; displacement of the graft; material fatigue and degradation over time; graft limbs or tubes that were too short or that ended in the distal cone of the aneurysm; a size mismatch between the graft limb and the vessel. In all these patients additional stents must be implanted to seal the leaks [4].

It is also important to note that not all patients are suitable candidates for stent-grafts insertion procedure, primarily due to anatomic features that cannot be accommodated by current stent-graft designs [5].

From the above discussion on the peculiarity of patient disease, the need to produce custom stent-grafts, emerges. Surgeons agree that this customization allows a reduction of global cost, and time-length extension [6]. An important goal of the stent-graft customization procedures is to build a good lumen replica which can be used as make-up model.

The main goal of this work is to obtain an accurate and suitable shape representation of a lumen vessel that can be automatically manufactured in order to help such a customization. To achieve such kind of customization process we reconstruct a valid solid model of vessels from CT data, and after a preliminar medical validation we make a 3D printing of it using the RP technique known as Fused Deposition Modelling (FDM).

In general RP refers to the physical modelling using a special class of machine technology. Using an additive approach to build shapes, RP systems join liquid, powder or sheet materials to form physical objects layer by layer using thin, horizontal cross sections of the computer model [7].

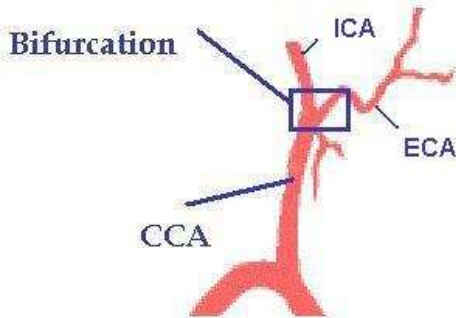


Fig. 1. Our region of interest is the carotid region enclosed by the bold-face rectangular. Common Carotid Artery (CCA), Internal Carotid Artery (ICA) and External Carotid Artery (ECA), with bifurcation are graphically represented.

The most complex point of the shape reconstruction is the bifurcation region, we are dealing with the common carotid artery. The human carotid artery bifurcation is a complex, three-dimensional structure exhibiting non-planarity and both in- and out-of-plane curvature [8].

Our specific objectives were:

- to write a rapid and automatic routine for lumen segmentation and surface reconstruction from serial CT images;
- to have as much control as possible of the manufacturing pipeline of the lumen vessel;
- to produce a 3d printing of the solid model of the vessel with FDM technique.

Main reconstruction methods present in literature are based on:

- Stereoscopic algorithms;
- Balloon algorithms;
- CAD reconstruction from serial images from CT or MR (Magnetic Resonance)

Blondel et al. [9] illustrate an algorithm for an automatic 3D reconstruction of the coronary arteries centerlines from

three angiograms, taken from a single rotational stereoscopic acquisition. This approach recovers the geometry of the main arteries through the point matching in two of the segmented images using the information recovered from the third image. This method needs good calibration and requires breatheld acquisitions.

Yoo et al. [10] present the use of variational surfaces for anatomic modelling. From data acquired using an endovascular ultrasound transducer. The transducer is drawn slowly through the vessel acquiring cross-sectional images. Each individual slice is then segmented and the aggregate contours are processed to form a variational implicit surface. It is a method that allows the employment of sparsely and unevenly sampled data to represent complex biological surfaces. In addition the method represents easily shapes with arbitrary topology without interpolation or aliasing errors. However the computational cost of using this systems rise with the number of points required to faithfully represent the surface.

Wicker et al. [12] developed a geometric computer model by using two different commercial softwares. They were able to reconstruct accurate geometry of vessels for their use in RP process.

Ladak et al. [11] use a fast technique to extract arterial geometry, even from complicated branching geometries, from serial MR images. This result is carried out using a “virtual balloon” which, when placed inside the threedimensional lumen geometry given by the serial MR image data, is inflated to simultaneously segment and reconstruct the lumen. In some cases, the reconstructed surface may need to be manually modified.

Our work follows the scheme proposed by Ladak [11], but unlike his technique, we use an automatic shape reconstruction technique to reconstruct complex geometry and topology changes.

II. TOOLS AND METHODS

The project is developed according to the pipeline shown in Fig. 2.

There are three main steps:

- Shape acquisition from image segmentation;
- Shape reconstruction;
- Shape printing with FDM;

Each phase is analyzed below:

A. Shape acquisition from image segmentation

The dataset chosen for this study is an autoptic specimen of a human right carotid artery, fixed while distending to restore normal in vivo morphology, explanted from a cadaver of a 32 years old man, died by an accident, without apparent cerebral disease [17]. The examination was performed by a helical Picker scanner 5000 of the Brotzu Hospital in Cagliari. Dataset was transferred from the clinical device to our workstation by using DICOM3 standard protocol [18], [19].

The principal goal of a segmentation process is to partition an image into regions that are homogeneous with respect to one or more features. The application of segmentation yo our

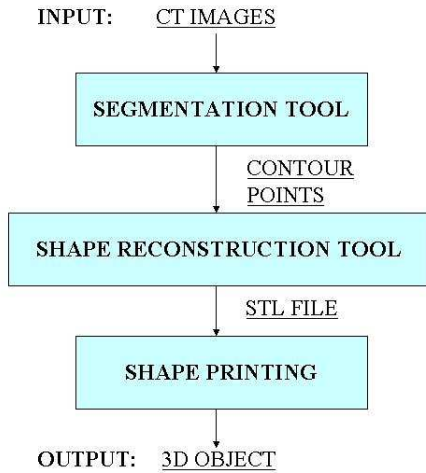


Fig. 2. The pipeline of lumen reconstruction and manufacturing project. The segmentation tool is the segmentation software written during VIVA [21] project, a previous project developed at CRS4. 3D printing of the object output from splinator is realized with FDM technique [24].

problem includes the lumen boundary detection, see Fig. (3). Principal approaches for edge and lines detection in an image are based on thresholding, region growing, region splitting and merging; a comparison between the segmentation techniques is out of the purpose of this article interested readers can refer to [13].

The picture segmentation is a semi-automatic process driven by the end-user (operator). We used the library *Contour* [20] developed during VIVA project [21] based on GSSNAKE [22] open-source software (the analysis of the segmentation algorithm details is described in [14]). Fig. (3) shows the final step of the segmentation algorithm applied on the original CT image of the vessel structure; each acquired CT image is segmented to have the 2D shape. Our approach is based on region growing algorithm, it starts with a pixel (seed) or a group of pixels that belongs to the lumen (shown in green in Fig. 3).

A simple reparametrization algorithm is applied to all points vectors ($J \in [0, n_{sld}]$, where n_{sld} is the number of CT slices) in order to simplify the shape reconstruction task. All points at cross level J are parameterized in clockwise order starting from the minimum $x_{coordinate}$. The corresponding point in the adjacent image plane curve ($J+1$), is found by nearest distance computation between points belonging to two adjacent slices.

B. Shape reconstruction

The solid model of the carotid lumen is made using Boundary Representation (BRep). B-Rep models describe a solid indirectly by representing its bounding surface [25]; they can be used for a wide class of objects but for objects with a complex data structure, they require a large memory space [26]. To avoid troubles during the data-processing phase before 3D printing, we need to compute a valid BRep Model, i.e. a model fulfilling the following conditions: the set of faces must form a complete skin of the solid with no missing parts, faces

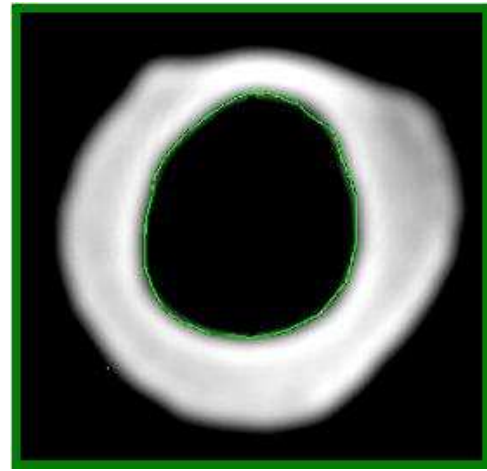


Fig. 3. Autoptic carotid CT image segmentation. Pixel dimension are $7.810^{-2}mm$ for x and y coordinates, while the slice width is 2 mm; the distance between two adjacent slices is 3 mm. The lumen (black region) boundary has been identified by a region growing algorithm. The result is a set of points (green color). The CT image has a resolution of 512 x512 pixels.

must be closed, coherently oriented, bounded, connected, and must not intersect each other except at common vertices or edges [27]. We resolved these problems using Open Cascade, and Qt for visualization.

1) *Open Cascade*: **Open Cascade** [28], or simply OCAS, by MATRA is a general-purpose CAD (Computer Aided Design) software. This system gives a complete application development environment, made up of about 10.000 classes written in C++ and organized in about 400 project files. In particular, an "OCAS project" is a collection of classes that share common functionalities in some semantic area of geometry and/or graphics.

The classes of OCAS offer the infrastructure (*Rapid Application Framework*) either for both the rapid development of geometric computing oriented applications and for "design" in some specific areas of interest, say in advanced CAD tools, design databases, simulation systems or graphics rendering of complex assemblies.

OCAS internal code organization uses only C++ *classes* that are grouped under *packages*. Every package belongs to an OCAS *library*; finally a group of libraries forms a *module*. The main reason of this software architecture is to link together services and algorithms which operate in the same semantic domain.

OCAS provides a smart pointer mechanism called **handle** which allows automatic memory management.

2) *QT*: **Qt** [29] is a multiplatform C++ GUI application framework. It provides application developers with all the functionality needed to build applications with state-of-the-art graphical user interfaces. Qt is fully object-oriented, easily extensible, and allows true component programming. Qt structure matches perfectly with OCAS structure.

C. Shape printing with FDM

The solid reconstruction of the carotid lumen in each of the above specimens, is exported in STL format, and transmitted to the prototyping device. We use a RP machine with FDM technique. FDM is a technique whereby digital surface models are converted to scale models of resin or wax. It works with STL representation of solid objects and the main steps of its pipeline are: acquiring the STL file; orienting it in the right position in order to satisfy some constructive needs; slicing the STL geometry obtaining a set of sections which can be thought as level curves of the object; 3D printing [23]. This task is performed by the *Quickslice* (©Stratasys) program furnished with the 3D printer.

III. DISCUSSION

After interpolation and reparametrization tasks, the result for each vessel section is a closed B-spline curve [30], 128 generating 3D points are enough to represent the 2D lumen. The points vector obtained represents the geometric constraints for the generating interpolation curve. The points interpolation procedure of single arrays is realized with one B-Spline curve for each slice. B-Spline curves provide sufficient control flexibility for the scope of the application, we can use lower degree curves and still maintain a large number of control points. Since B-spline curves satisfy the strong convex hull property, they have a fine shape control. In particular a position change of a control point does not globally affect the shape of the whole curve (local modification property). As described previously, for each cross section we have a finite number of closed contours which represent sections of vessels. By using OCAS geometry tools it is possible to connect two closed parameterized B-splines belonging to two adjacent cross sections (levels), obtaining a B-spline surface which can be thought as a portion of a cylinder. This task is carried out by connecting curves of adjacent levels in a one-to-one mapping between the points of a curve with points of the other one. The OCAS commands used to perform the process is the following:

```
Cx=GeomAPI_Interpolate
(const Handle(TColgp_HArray1OfPnt)& Pnts,
 const Standard_Boolean PeriodicFlag,
 const Standard_Real Tolerance)
```

Where *Pnts* is the points vector given by the segmentation algorithm. **GeomApi_interpolate** class initializes an algorithm for constructing a constrained BSpline curve passing through the points of the table *Pnts*. If *PeriodicFlag* is set to true, the constrained BSpline curve will be periodic and closed. In this case, the junction point is the first point of the table *Pnts*. The tolerance value *Tolerance* is used to check that points are not too close to each other, or tangential vectors (defined using the function *Load*) are not too small. We set this value to *Tolerance=1.0e-3* (two order of magnitude lower than the pixel size). The resulting BSpline curve is "C2" continuous. The method **IsDone()** checks the validity of the interpolation

result and the method **Curve()** returns the computed B-Spline curve (Fig. 4).

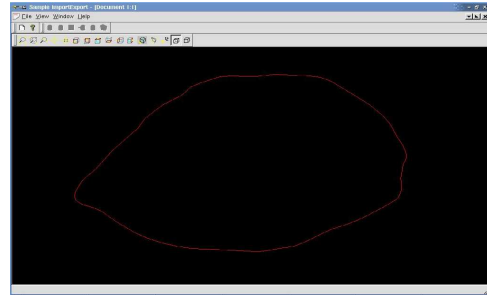


Fig. 4. Points on each single slice are interpolated by using a B-Spline periodic and closed curve.

To connect the B-Spline curves obtained during the previous step we use B-Spline surfaces, surface properties are similar to curves properties. The key characteristic of these surfaces is that they are parametric. Note that all surfaces must have a geometric continuity, and any surface is at least "C0". Generally, continuity is checked at construction time or when the curve is edited. OCAS makes this explicit at execution time. The class:

```
Sx= GeomFill_BSplineCurves
(const Handle(Geom_BSplineCurve)& C1,
 const Handle(Geom_BSplineCurve)& C2,
 const GeomFill_FillingStyle Type)
```

constructs a framework for building a BSpline surface from the two contiguous BSpline curves, C1 and C2; *Type* is an attribute indicating the style of the surface, in our case is a rounded style of patch. The alternatives are "flat patches", or "more rounded patches". From each B-Spline surface we create a Shell, i.e., a shape corresponding only to the skin and not to a solid model defined by a boundary and a thickness (see Fig. 5 b). As the surface is "C2" continuous, the shell contains only one face. The OCAS class is:

```
Sh = BRepBuilderAPI_MakeShell shellgenoff
(Sx.Surface());
```

After the shell sequence production, we create the solid made of a series of shells which do not intersect each other. One of these shells constitutes the outside skin of the solid. There is not an OCAS method during the construction of solid to verify that shells does not intersect each other (Fig. 5).

Reconstruction problems arise when topological structure of cross sections changes when passing from a section to the subsequent. A case of topological change is the *bifurcation* (see Fig. 6)

Our aim is to develop an automatic method to manage this problem, i.e. to connect two tubes with a single one. It is not a simple task to connect a set of plane sections when they pass from one to two closed contours. The one-to-one mapping of vertices described above is no longer possible.

Antiga et al. [16] technique use segmented lumen vessel verteces and extract shape structures by an axial sectioning.

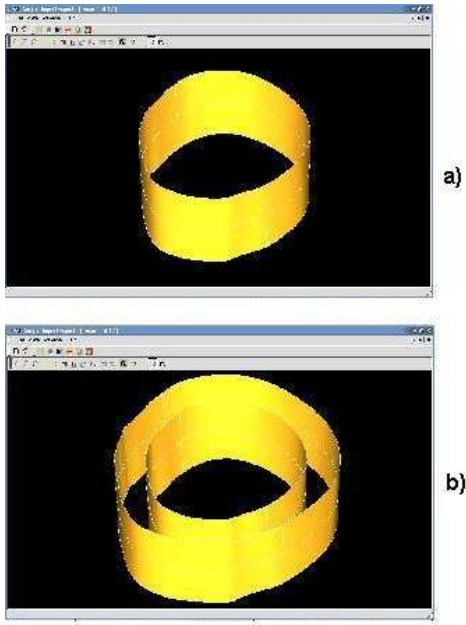


Fig. 5. a) Junction shell of 2 contiguous B-Spline curves. The B-Spline surfaces are joined to form the lumen vessel. b) Internal and external parallel shells are necessary to create a printable solid. The outer surface is an offset surface of the inner one.

The topological problem at bifurcation regions is solved by gluing two triangular patches to fill the holes generated by the junction of the three cylindrical portions, as shown in Fig. 7.

This solution requires the computation of the curve reconstruction algorithm to the images from CT dataset, perpendicularly to the axial centerline. The axial centerline is computed in a previous step and after the image interpolation process; it is necessary to extract the new centerlines aligned images from the volume dataset (the stack of CT images). At the end a new segmentation step is applied to extract the new generating curve of the bifurcation.

While looking for the most suitable solution for reconstructing the carotid region lumen shape, we also tried a four parts decomposition technique shown in Fig. 8. The four patches LFS, RFS, LBS and RBS (LFS is the acronym of Left Front Surface, etc.) were obtained by cutting the region of interest with two vertical planes passing through a point belonging to the bifurcation region (the apex point P_5 in Fig. 8 b). One of the vertical planes is the bifurcation plane (sagittal plane), the other one is perpendicular to it (transaxial plane). This kind of decomposition was not suitable for the following reasons:

- greater is the number of patches to be joined, more complicated is the joining surface blending operation.
- referring to figure 8: each of the four patches into which the object is decomposed is bounded by five curves (referring to LFS: $P_7 - P_2, P_2 - P_5, P_5 - P_3, P_3 - P_6, P_6 - P_7$), two of which ($P_7 - P_2$ and $P_3 - P_6$) belong to transaxial planes, $P_2 - P_5$ belongs to sagittal plane and $P_5 - P_3$ and $P_6 - P_7$ lie on coronal plane.

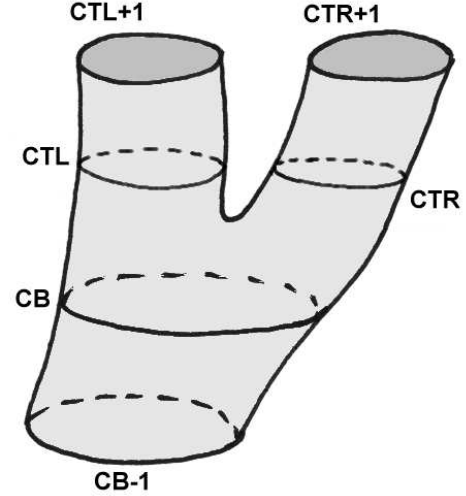


Fig. 6. Simplified representation of the carotid vessel. The end of CCA part made of the curves CB-1 and CB is connected to the bottom part of ECA (defined by the lumen curves CTR and CTR+1) and to the bottom part of ICA (defined by the lumen curves CTL and CTL+1).

This means that we should define the vertical curves separately, with the extreme points being the only known data about them. Moreover, even with the well-defined bounding curves (we tried using circle and parabola segments passing by P_3, P_5, P_1 and P_2, P_5, P_4), they are not sufficient to generate an acceptable B-spline surface: point-to-point coincidence between different patches is not guaranteed on border curves and reconstruction operation failed near the vertices of bounding curves.

We demonstrate now that is possible to solve the bifurcation shape reconstruction automatically by using only parallel serial shape curves (the curves CTL, CTR, CB shown in Fig. 6)

We divided the bifurcation region into three parts (as shown in Fig. 9), which are quadrilateral parametric surface patches. Then we reconstruct the B-spline surface for each one of the three patches, and join them to form a single surface.

To obtain the surfaces we select the points P_3 and P_4 respectively on the curves CTL and CTR of Fig. 9. P_3 and P_4 are the extreme-points, belonging to the original arrays, of the minimum distance segment between the two curves CTL and CTR. Then we calculate the segment perpendicular to segment $P_3 - P_4$, passing through its medium point and translate it on CB plane. This point must belong to the region bounded by CB, P'_5 that is inside the region bounded by CB is a good candidate. Then, on curve CB, we take the points P_1 and P_2 , belonging to the original segmented vector points array. Such points are the nearest points to the intersection points between CB and segment perpendicular to segment $P_3 - P_4$. We divide the array CB into two open arrays, CBL and CBR on Fig. 9. Open arrays are needed as supports to overcome the difficulties given by the topological change passing from slices with one contour to slices with two different contours. To obtain the

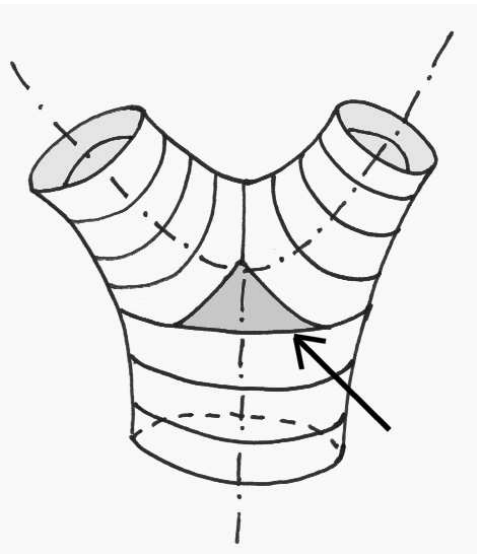


Fig. 7. Geometric solution of the carotid bifurcation problem: Antiga approach. Two triangular patches are glued to the three cylindrical portion, the arrow points to the front added triangulated shape surface patch.

lateral surfaces of the bifurcation, we connect CBL with CTL and CBR with CTR still using the OCAS class:

```
Sx= GeomFill_BSplineCurves
  (const Handle(Geom_BSplineCurve)& CBL,
   const Handle(Geom_BSplineCurve)& CTL,
   const GeomFill_FillingStyle Type)
```

After this job, a quadrilateral hole remains to be filled in the middle of the object. It can be closed with a third quadrilateral saddle-like patch (Fig. 9), obtained again with the same class *GeomFill_BSplineCurves* having as arguments the B-Spline right curves identified by EFL and EBR.

```
Sx= GeomFill_BSplineCurves
  (const Handle(Geom_BSplineCurve)& EFL,
   const Handle(Geom_BSplineCurve)& EBR,
   const GeomFill_FillingStyle Type)
```

Joining the B-Spline surfaces obtained connecting open arrays with the central B-Spline surface, we obtain a single surface of bifurcation (Fig. 10).

At the same time we reconstruct an external skin for the solid model of the lumen vessel; the resulting external shell is parallel to the internal one.

The program ends its work exporting the obtained solid shape in a file written in STL (STereoLitography) format. STL is the input format accepted by all RP devices and hence by FDM 2000 device, our 3D printer. The OCAS class used is:

```
Stlwriter= StlAPI_Writer();
Stlwriter.SetDeflection
  (const Standard_Real aDeflection);
Stlwriter.SetCoefficient
  (const Standard_Real aCoefficient);
Stlwriter.Write(SHAPE,shape.stl);
```

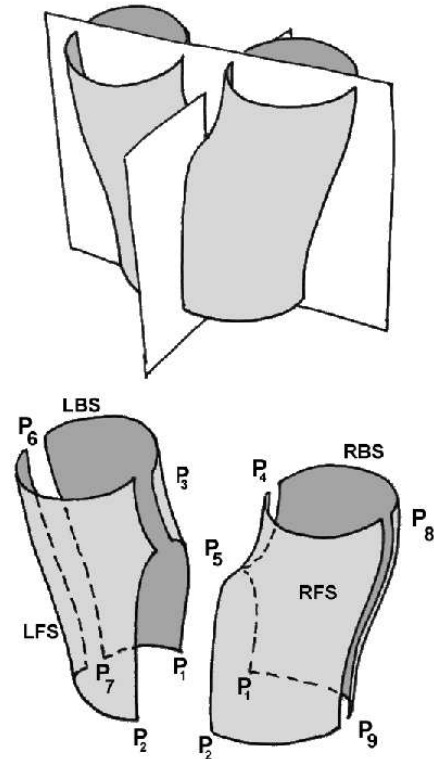


Fig. 8. Shape reconstruction of the bifurcation: Deleo approach. Four patches are created and joined to obtain a surface. The curves (P_3, P_4, P_5) and (P_2, P_5, P_1) are computed automatically imposing the points constraints to circle curves.

By changing values of *aDeflection* and *aCoefficient* we can affect the number of triangles of the resulting mesh. The deflection represents the maximum distance permitted between any point on the surface and the corresponding point on the triangulation.

The output shape can be inspected interactively before to be (directly) exported in the ultimate format for the RP device.

IV. CONCLUSION

With the prototypal system we set up, we were able to obtain a complete shape reconstruction and manufacturing of vessel structures starting from CT datasets. We applied the technique to a set of five autoptic data set. The shape reconstruction algorithm produces fit replicas of the lumen replicas (see Fig. 14). The tessellation automatically generated by OCAS classes is of poor quality, and unfitable with our needs. The reconstructed BRep model is valid and “CO”, but its tessellated version is not “CO”. Thin holes are present between the surfaces edges. this problem is not visible when the FDM producing layer is the same as the CT transaxial. At this moment we can not operate on triangle composition and directly on their dimension. A critical point is the size of output STL file which becomes very large to obtain a perfect match between triangulation representation and lumen

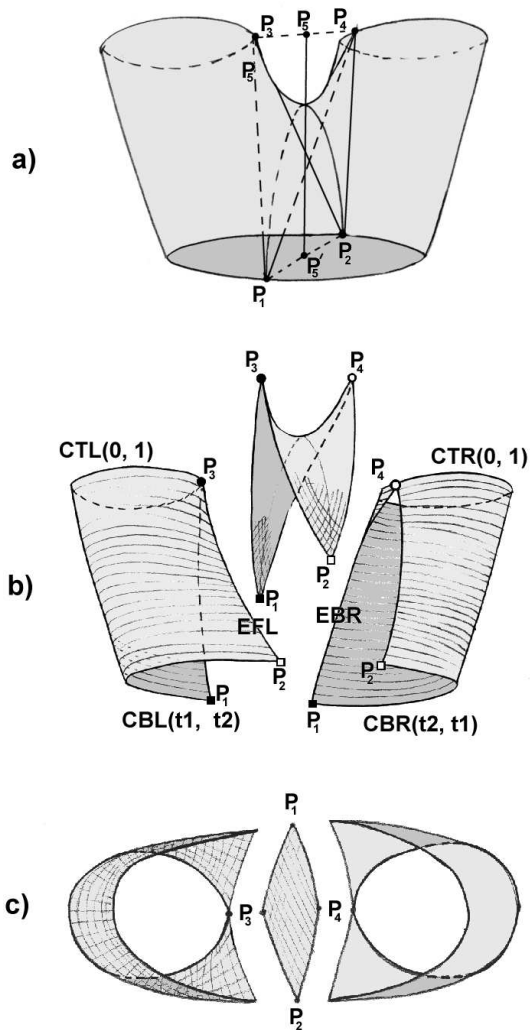


Fig. 9. a) and b) Decomposition of a bifurcation region in three quadrilateral patches. c) Top view. The generating curves for the third patch are automatically computed from the point P_5 which is selected by the point P_3 and P_4 belonging to the crossed planar curve.

geometrical description About the chosen bifurcation region algorithm for shape reconstruction, it has the advantage of being quite simple, hence easily implemented, and it only involves parts of planar horizontal curves and linear edges segments (EFL and EBR in Fig. 9) as generating curves for the third B-spline patch, which means that no added data have to be introduced (no centerline curves neither non-parallel edges are necessary). Moreover, dealing exclusively with parallel curves, obtained straight from CT image by any segmentation algorithm, presents the further advantage that we can immediately compare the image processing segmentation results with the manufacturing slices used by RP devices (as shown in Fig. 12). Such a technique is the final tool to evaluate the quality of the lumen replica.

This approach can solve the simplest bifurcation case, the



Fig. 10. Generation of three patch-shells for bifurcation. The three B-Spline patches resulting from the automatic shape reconstruction algorithm.

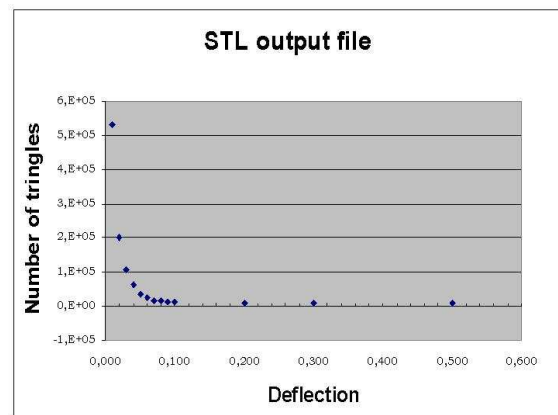


Fig. 11. This histogram shows the relationship between the value of the deflection (mm) and the number of triangles generated from to OCAS tessellation algorithm. As the deflection becomes lower than 0.03 mm the number of triangles overcomes the threshold of 10^5 .

case of a vessel tube which is splitted in two parts. This is not the only case in which a bifurcation can appear. Fig. 13 shows the case of a vessel portion in which a single tube splits into two ones and its lumen cross sections is more complicated then the example we have presented. This case can be solved coupling topological tools (see [31] for a complete survey of how managing general topological changes)

According to literature and market data, the cost of the stent graft is approximately \$600 making use of open surgery and \$7,000 making use of endovascular repair. On the basis of these estimates from the literature, stent graft disposal costs represents respectively about 34% ($\$7,000/\$20,716$) and 3% ($\$600/\$18,484$) of the total procedural costs for endovascular and open surgical repairs [32].

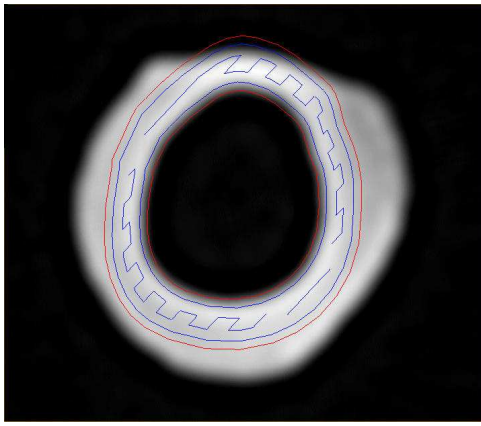


Fig. 12. Building up the test case of lumen replica. The image shows the correspondence between the CT image (background image), and the simulation of the building job: the red curves represent the section of the STL, while the blue ones are the tool-paths to be covered by the FDM machine in order to fill the section with building material. This image has been obtained overimposing the output of the Quickslice ©(Stratasys) program used by FDM device.

Our tool is entirely written with open source software (OSS), which means versatility, independence from commercial software, hence affordability for economically weak Institutions [15], this features guarantee that the radiologist has a total control over each step of the pipeline. The software can be customized to the user's needs, either adding new classes and methods or changing the involved parameters. Last but not least point is that OSS is free, which means a considerable reduction of costs for hospitals.

V. FUTURE WORK

This is a work in progress. We are going to apply this technique to a set of five autoptic clinical cases. Evaluation from a medical point of view will be performed to test the quality of the reconstruction step. This operation will be carried out by a medical team, which will compare virtual reconstructions and material replicas with real parts on a survey of clinical cases. Also, future developments of this work will be devoted to make completely automatic the whole pipeline from the segmentation step till to the FDM printing, which at this moment involves some tasks (in the segmentation step) to be done by the operator. Because the stl slicer of quickslice works better if the triangles are small and equilateral, the capability of managing meshes will be an important task of futur work.

ACKNOWLEDGMENT

This research was supported by the Italian Government MIUR and by the Local Sardinian Authorities which cofunded the Laboratory for Advanced Planning and Simulation project. The medical datasets were provided by the Radiology and Vascular Surgery Dept. of the Brotzu Hospital of Cagliari, Italy. Thanks to Dr.ssa Grazia Bitti (MD), Dr. Gildo Matta (MD) and Dr. Paolo Schifflini (MD) of Brotzu Hospital for the radiological acquisition. The authors would like to thank also Dr. Andrea Giachetti, Dr. Alan Scheinine of CRS4 for

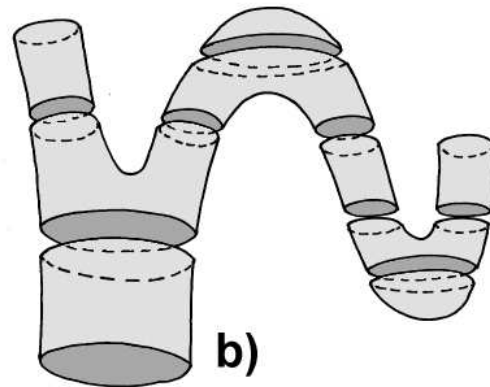
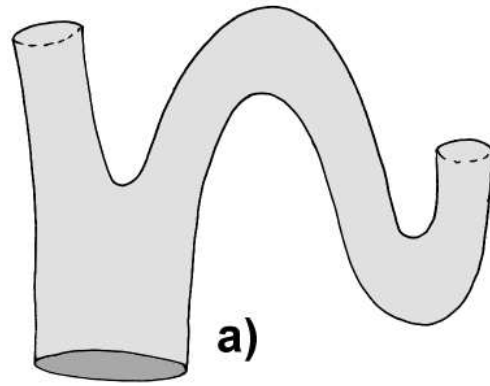


Fig. 13. Possible geometric shape of a carotid vessel (a): the maximum number of closed curves can be larger than two which is the number considered in this work. Three bifurcations and two caps connected by tubes as shown in (b).

providing the image segmentation tools. Thanks to Ing. Andrea Costaglioli and Ing. Mikreyt Clementini of PROTO21 for their support in manufacturing the replicas.

Thanks to Helga Wilson-Massidda for her fundamental support and her assistance on writing this paper.

REFERENCES

- [1] Parodi JC and Palmaz JC and Barone HD. *Transfemoral intraluminal graft implantation for abdominal aortic aneurysms*. Ann Vasc Surg 1991; 5:491-499
- [2] Greil O. and Pflügbeil G. and Weigand K. and Weiss W. and Liepsch D. and Maurer PC. and Berger H., *Changes in carotid artery flow velocities after stent implantation: a fluid dynamics study with laser Doppler anemometry*. Journal of Endovascular Therapy. 2003 Apr;10(2):275-84.
- [3] Kaufman J. A. and Geller S. C. and Brewster D. C. and Fan C.M. and Cambria R. P. and LaMuraglia G. M. and Gertler J. P. and Abbott W. M. and Waltman A. C., *Endovascular Repair of Abdominal Aortic Aneurysms: Current Status and Future Directions*. AJR 175: 289-302
- [4] M. Tillich and K. A. Hausegger and K. Tiesenhausen and J. Tauss and R. Groell and D. H. Szolar, *Helical CT Angiography of Stent-Grafts in Abdominal Aortic Aneurysms: Morphologic Changes and Complications* Radiographics. 1999;19:1573-1583
- [5] Duda SH. and Raygrotzki S. and Wiskirchen J. et al., *Abdominal aortic aneurysms: treatment with juxtarenal placement of covered stent-grafts*. Radiology 1998;206:195-198.



Fig. 14. Finals shape reconstructed lumen replica, produced in ABS resin. The number of CT slices is forty-six. A deflection parameter of 0.01 mm is used to tessellate about five hundred thousand triangles. The RP manufacturing time was seven hours.

- [6] AA. VV., *The future of medical technology: improving patient outcomes and reducing costs*. Health Industry Manufacturers Association, Vol. 1(8), 2000.
- [7] T. Wohlers *Wohlers report - Annual Worldwide Progress Report*. Wohlers Associates, 2002.
- [8] Thomas JB. and Milner JS. and Steinman DA., *On the influence of vessel planarity on local hemodynamics at the human carotid bifurcation*. *Biorheology*. 2002;39(3-4):443-8.
- [9] Blondel C. and Vaillant R. and Devernay F. and Malandain G. and Ayache N., *Automatic trinocular 3D reconstruction of coronary artery centerlines from rotational X-ray angiography*. *Computer Assisted Radiology and Surgery* 2002 Proceedings, 2002. Springer Publishers, Heidelberg.
- [10] T. Yoo and B. Morse and K. R. Subramanian and P. Rheingans and M. Ackerman, *Anatomical Modeling from Unstructured Samples Using Variational Implicit Surfaces* *Medicine Meets Virtual Reality*. IOS Press, 2001.
- [11] Ladak HM and Milner JS and Steinman DA. *Rapid three-dimensional segmentation of the carotid bifurcation from serial MR images*. *Journal of Biomechanical Engineering*. 2000 Feb;122(1):96-9.
- [12] R. Wicker and M. Cortez and F. Medina and G. Palafox and C. Elkins, *Manufacturing Complex Compliant Cardiovascular System Models for In Vitro Hemodynamic Experimentation Using CT and MRI Data and Rapid Prototyping Technologies*. *ASME Bioengineering Division (BED) Volume 50*, 2001, pp. 469-470.
- [13] R. C. Gonzales and R. E. Woods, *Digital Image Processing*. Addison-Wesley, 1993.
- [14] AA. VV, *HandBook of Medical Imaging: Processing and Analysis*. Bankman - Academic Press, 2000.
- [15] AA. VV., *Open Sources: Voices from the Open Source Revolution*, Di Bona, Ockman, Stone editors. 1999.
- [16] L. Antiga and B. Ene-Iordache and L. Caverni and G. Cornalba and A. Remuzzi, *Geometric reconstruction for computational mesh generation of arterial bifurcations from CT angiography*. *Computerized Medical Imaging and Graphics*. 2002; 26: 227-235.
- [17] E. Gobbetti and P. Pili and A. Zorcolo and M. Tuveri, *Interactive Virtual Angioscopy*. *Proc. IEEE Visualization 1998* (1), pp. 435-438.
- [18] A. Giachetti and M. Donizelli and A. Scheinine, *DICOM image handling for medical analysis and the ViVa Project*. *Proceedings of EuroPACS '98* (1), pp. 117-120.
- [19] D. A. Clunie, *DICOM Structured Reporting* PixelMed Publishing, 2001.
- [20] A. Scheinine and M. Donizelli and M. Pescosolido, *An object-oriented client-server system for interactive segmentation of medical images using the method of active contours*. *Proceedings des Workshops Bildverarbeitung fr die Medizin 1998*, Springer Verlag.
- [21] G. Abdulaeev and S. Cadeddu and G. Delussu and M. Donizelli and L. Formaggia and A. Giachetti and E. Gobbetti and A. Leone and C. Manzi and P. Pili and A. Scheinine and M. Tuveri and A. Varone and A. Veneziani and G. Zanetti and A. Zorcolo, *ViVa: the Virtual Vascular Project*. *Information Technology in Biomedicine*, pp. 268-273, December, 1988.
- [22] K. F. Lai and R. T. Chin, *Deformable Contours: Modeling and Extraction*. *IEEE Trans. Pattern Anal. and Machine Intell.*, 1995 17(11), pp.1084-1090.
- [23] P. Pili and F. Murgia and G. Pusceddu and G. Franzoni *Physical lumen carotid reconstruction: life-size models by Rapid Prototyping*. *Physiology and function: Methods, Systems and Applications - Medical Imaging 2003 - Proceedings of SPIE*, Vol. 5031. 2003.
- [24] A. Gatto and L. Iuliano, *Prototipazione Rapida*. *Tecniche Nuove*, 1998.
- [25] M. MANTYLA, *Solid Modelling*. Computer Science Press, 1995.
- [26] Sulkimo J. and Vuoskoski J., *Particle Tracking in Sophisticated CAD Models for Simulation Purposes*. *Nucl. Instr. Meth. Phys.Res.A.* - 371 (3), pp. 434-438", 1996.
- [27] M. MORTENSON, *Geometric Modeling*. Wiley and Sons, 1997.
- [28] AA. VV., *Open Cascade, Foundation classes. User's Guide* EADS Matra Datavision, 2001.
- [29] M. K. Dalheimer, *Programming with Qt*. O'Reilly, 1999.
- [30] G. Farin, *Curves and Surfaces for Computer Aided Geometric Design - A Practical Guide, 3rd ed.*. Academic Press, 1993.
- [31] A. T. Fomenko and T. L. Kunii, *Topological modeling for visualization* Tokyo Springer, 1997.
- [32] J. L. Bosch and J. S. Lester and P. M. McMahon and M. T. Beinfeld and E. F. Halpern and J. A. Kaufman and D. C. Brewster and G. Scott Gazelle, *Hospital Costs for Elective Endovascular and Surgical Repairs of Infrarenal Abdominal Aortic Aneurysms1* *Radiology*. 2001;220:492-497.